MANGANESE-DEOXYRIBONUCLEIC ACID BINDING MODES

Nuclear Magnetic Relaxation Dispersion Results

SCOTT DOUGLASS KENNEDY AND ROBERT G. BRYANT
Department of Chemistry, University of Minnesota, Minneapolis, Minnesota 55455

ABSTRACT Ion-DNA interactions are discussed and the applied magnetic field strength dependence of water proton spin-lattice relaxation rates is used to study the Mn(II)-DNA interaction both qualitatively and quantitatively. Associations in which the manganese II (Mn(II)) ion is completely immobilized on the DNA are identified as well as a range of associations in which the ion is only partially reorientationally restricted. Quantitative analysis of the strength of the association in which manganese is immobilized is carried out both with and without a counter-ion condensation correction for electrostatic attraction of the mobile ions. From competition experiments with manganese the relative strengths of the interactions of magnesium and calcium with DNA are found to be identical but less than that of manganese with DNA and the affinity of lithium for DNA is found to be slightly higher than that of sodium. The data demonstrate that the reduced mobility of nonsite-bound ions may have a significant effect on DNA-ion binding analyses performed using magnetic resonance and relaxation methods.

INTRODUCTION

Much remains to be learned about the details of the metal ion involvement in the control and regulation of critical biochemical processes. An interesting aspect of metal binding to macromolecular systems is the interplay between the long range electrostatic forces, which may lead to double layer phenomena at charged surfaces for example, and much stronger chemical bonding interactions that involve the first coordination sphere of the metal at very short range. The question of long range electrostatic binding vs. first coordination sphere binding, which we take as two useful extremes, has been studied at length for monovalent and divalent ions binding to DNA, considered in this case as a model for a rigid charged rod. There is no evidence from either theory or experiment that the binding of sodium ion for example to DNA involves a significant perturbation of the sodium ion first coordination sphere. That is, the ion binds as a fully solvated species, and the binding interaction is thus dominated by long range electrostatic interactions. Though divalent ions are known to associate with DNA and affect a number of its physical characteristics such as thermal stability, the chemistry of divalent metals is rich and the involvement of different or multiple binding modalities is possible. In addition divalent metal binding may affect the interaction of DNA with other molecules, including those involved in the transcription process. Thus, a mechanistic understanding of metal involvement in mutagenesis requires a clear view of the metal binding events.

Magnetic resonance methods have often been applied to this problem with the hope of both a structural and dynamical characterization of the bound metal ion state. Thus far, direct observation of metal resonances has failed to provide satisfying quantitative data on binding, though in contrast to the monovalent ions there is clear evidence for significant involvement of first coordination sphere binding interactions (1). Though much less direct, proton nuclear magnetic relaxation spectroscopy has been used to quantitate metal binding and distinguish between major categories of bound ion (2). Manganese(II) (Mn(II)) is particularly useful because of its magnetic properties, though its chemical similarity to other divalent metals common to the intracellular environment may be questioned. In addition proton magnetic relaxation enhancement is often assumed, without justification, to be sensitive to tight binding of the Mn(II) ion. We report here an extensive study of the water proton magnetic relaxation rate measured over a wide range of magnetic field strengths that addresses the assumptions of the experimental approach and provides important quantitative data on the interactions of this divalent ion with native DNA. We address a definition of bound ion, specific features of the quantitative analysis of the magnetic relaxation data, quantitative results for manganese(II)-DNA binding, and metal ion competition experiments.

Dr. Kennedy's and Dr. Bryant's present address is Departments of Biophysics and Radiology, University of Rochester Medical Center, P.O. Box 648, 601 Elmwood Avenue, Rochester, New York 14642.

EXPERIMENTAL DETAILS

Calf thymus DNA was obtained from Millipore Corporation. ~120 mg of DNA was placed in vials at room temperature filled with 20 ml of a stock salt and buffer solution containing 10mM tetrabutylammonium chloride (Bu_4NCl), 1mM tris buffer (pH 7.8), and 0.1 mM sodium azide and left for 2 d at 5°C until the solution was uniform. To remove all traces of divalent ions, the concentrated solution was dialyzed for 10 h in a cold room against a constantly stirred one liter solution containing 5 mM ethylenediaminetetraacetic acid (EDTA) in addition to the stock salt and buffer. To expel EDTA, the DNA solutions were dialyzed in the same bags against one-liter volumes of stock salt and buffer solution for 6 h in each of four changes. The resulting DNA stock solution was stored frozen until use.

The concentration of the DNA solutions was determined on a monomer unit basis by UV absorption at 260 nm using a Cary 17-D spectrophotometer assuming a molar extinction coefficient 7,000 M^{-1}. The DNA was checked for denaturation by the absorbance ratio at 260 nm for pH 8 and pH 12. If A (pH 12)/A (pH 8) > 1.28 the sample was considered acceptable for experiments. The pH of all DNA solutions was found at the beginning and end of each titration series to be between 7 and 8.

Manganese chloride ($MnCl_2 \cdot 6H_2O$) and magnesium chloride ($MgCl_2 \cdot 6H_2O$) (MC&B Manufacturing Chemists, Inc., Plainfield, NJ) calcium chloride (anhydrous) from Spectrum Chemical Mfg. Corp., and tetrabutylammonium chloride from Aldrich Chemical Co. were all reagent grade and used without further purification. The concentration of the manganese stock solutions was determined by heating them with KIO_4 and H_2SO_4 to form permanganate followed by absorbance measurements at 525 nm, assuming an extinction coefficient for permanganate of $2.45 \times 10^3\ M^{-1}$.

Mn(II) titrations of DNA were performed by adding microliter aliquots of 10–500 mM stock solution to one-milliliter volumes of DNA solution, and the sample stirred at a low speed on a vortex mixer for 15–30 s. 5–10 min were allowed before relaxation measurements were made, although no dependence of the relaxation rates on equilibration time was observed. Tetrabutylammonium chloride was used as the supporting electrolyte solution because its affinity for DNA is low (3).

Data points were fitted to theoretical curves using a nonlinear least-squares simplex search routine on a VAX-11-780 computer. Other calculations and numerical analyses were performed on an IBM 5100 computer using APL.

Nuclear magnetic relaxation dispersion measurements were made using a field cycling instrument constructed in this laboratory in collaboration with Dr. S.H. Koenig and R.D. Brown, III of the IBM Watson Research Laboratories and described previously (4).

THE BOUND STATE

Conceptually, binding of an ion to a macromolecule may take several forms. At one limit the ion may participate in an intimate association with specific functional groups on the macromolecule such that there is a direct chemical bond between an atom or atoms of the macromolecule and the associated ion. In this case the distance between the interacting partners is too short to permit solvent to intervene. Thus, the complex could be called an intimate or contact ion pair or a first coordination sphere complex. The dynamical consequences of the association reaction must be that for the lifetime of the association the bound ion moves with the slow correlation time of the macromolecule; although if only one contact point is made, rotation of the complex about the unique point is possible. A second class of bound ion is one that maintains a full compliment of solvent in the first coordination sphere, but makes second coordination sphere hydrogen bonds to functional groups on the macromolecule. In other words this would be a solvent shared ion pair. The dynamical consequences of this outer sphere association could be similar to those for the first case: in either instance the reorientational correlation times for the solvent protons in the bound aquoion complex are longer than for those in an aquoion free in the bulk solution. It is important to point out that the solvent magnetic relaxation properties may not distinguish between these bound states, though relaxation measurements that exploit either contact or magnetic dipolar interactions between the binding ion and nuclei associated with the binding functionality of the macromolecule may (5). A third class of bound states are those where a full compliment of solvent remains associated with the bound ion without second sphere hydrogen bonds. The binding is thus long range and driven by electrostatic interactions. Such bound ions have been called territorially bound, domain bound, and condensed. The dynamical consequences of such binding are minor; the bound ion may move along the charged macromolecule essentially without restriction, impeded only by the local collisions, i.e. a local surface viscosity associated with transport in the region close to the polyion. The Mn(II) ion in DNA solutions may, in principle, sample all three classes of environment. The rotational mobility of the metal ion is severely restricted in the first two classes and a relaxation dispersion spectrum like that shown in curve A of Fig. 1 is expected, where the maximum relaxation rate occurs at high frequency. Although this curve is calculated, it is representative of data obtained from macromolecules in solution with bound manganese ions. The territorially bound ion would yield a dispersion spectrum like that shown in curve B, shifted somewhat from the macromolecule free spectrum, shown in curve C, by changes in the local viscosity at the surface. Curve B can be obtained from sufficiently viscous, aqueous solutions of manganese ion

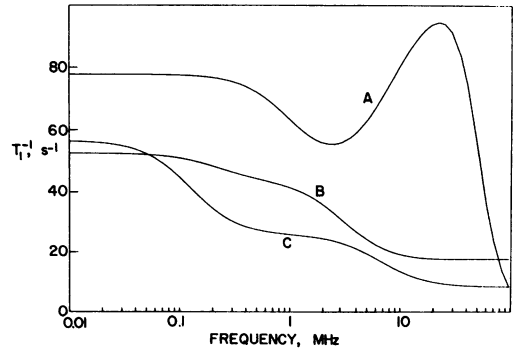

FIGURE 1 Nuclear magnetic relaxation rates of water protons obtained as a function of the applied magnetic field strength expressed as the Larmor frequency for (A) Mn(II) ion bound to bovine serum albumin; (B) Mn(II) ion in water-glycerol at 35 wt% at 286 K; (C) Mn(II) ion dissolved in water at 295 K. These curves were normalized to 1-mM Mn(II) concentration.

(6). The NMR dispersion spectrum is, therefore, capable of distinguishing tightly bound or immobilized ions from atmospherically bound ions though both types of bound ion decrease the activity of the free ion.

A number of analytical approaches are possible given a complete relaxation dispersion data set. For example Koenig and co-workers have measured the free manganese concentration in the presence of protein bound manganese by exploiting the magnetic field dependence of the free ion relaxivity at low fields where the bound ion contribution to relaxation is field independent (4). Alternatively, the large difference between bound and free curves at 20 MHz may also be exploited to measure the bound ion concentration (6). The observed data may also be fitted to the appropriately weighted sum of bound and free contributions using data obtained over the whole frequency range. We examine each of these approaches.

RESULTS AND DISCUSSION

Fig. 2, curve *A*, shows the magnetic field dependence of water proton relaxation in a solution containing 7.2 mM DNA and 0.03 mM $MnCl_2$. Several features are important: (*a*) Though the metal concentration is very low, the relaxation spectrum is field independent from 0.01 to 0.2 MHz; thus there is no evidence for the free ion. (*b*) The general shape of the dispersion plot is similar to the bound curve of Fig. 1, but the relative minimum is broader. (*c*) At 20 MHz, where the difference between bound and free ion relaxivity is greatest, the relaxation rate is high, clearly dominated by immobilized Mn(II) ions. (*d*) The shape of this dispersion is not a function of concentration in this region and may, therefore, be taken as representative of the bound state relaxation. At considerably higher concentrations of Mn(II) ion and lower concentrations of DNA, the dispersion curve changes shape as shown in Fig. 2, curve *B*, and the changes of the relaxation rate with field strength at low fields signals the presence of unbound Mn(II) ions.

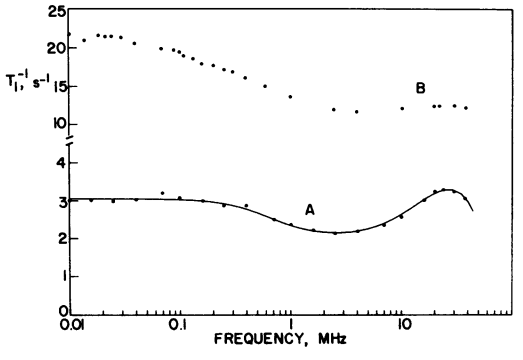

FIGURE 2 Nuclear magnetic relaxation rates of water protons obtained as a function of the applied magnetic field strength expressed as the proton Larmor frequency for (*A*) a 7.2-mM DNA phosphate solution containing 0.03 mM $MnCl_2$; (*B*) a 0.72-mM DNA phosphate solution containing 0.32-mM $MnCl_2$. Both data sets were obtained at 295 K. The solid line in Curve *A* was calculated from Eqs. 1–6 using the parameters listed in Appendix *A*.

The data of Fig. 2, curve *A*, were fitted to the theory of Solomon, Bloembergen, and Morgan (7–9), assuming a single environment and the parameters summarized in Appendix *A*. The paramagnetic contribution to the water proton relaxation rate in the aquoion is given by

$$\frac{1}{T_{1P}} = D\left[\frac{3\tau_c}{1+\omega_I^2\tau_c^2} + \frac{7\tau_c}{1+\omega_S^2\tau_c^2}\right] + E\left[\frac{\tau_e}{1+\omega_S^2\tau_e^2}\right], \quad (1)$$

where

$$D = (2/15)\gamma_H^2 g^2 \beta_e^2 S(S+1) r^{-6} \quad (2)$$

$$E = (2/3)(A/\hbar)^2 S(S+1) \quad (3)$$

and

$$\tau_c^{-1} = \tau_{ex}^{-1} + \tau_R^{-1} + \tau_S^{-1}; \qquad \tau_e^{-1} = \tau_{ex}^{-1} + \tau_S^{-1}, \quad (4)$$

where γ_H is the proton magnetogyric ratio, g is the electron Lande factor, β_e is the Bohr magneton, S is the electron spin, r is the intermoment distance, A is the electron-nuclear contact hyperfine coupling constant, and ω_I and ω_S are the angular Larmor frequencies of the proton and electron, respectively. τ_c is the correlation time for the electron-nuclear dipole-dipole interaction, τ_{ex} the mean residence time of a proton in the manganese first coordination sphere, τ_R the rotational correlation time for the intermoment vector, and τ_S the electron relaxation time given approximately by T_{1e} for most situations (10). The total observed water proton relaxation rate is the weighted average

$$1/T_1 = (1/T_{1a}) + \sum_i P_i/(\tau_{ex} + T_{1i}), \quad (5)$$

where P_i for the manganese sites is given by $q_i[\text{Mn(II)}]/[H_2O]$, where q_i is the number of water ligands per manganese ion in site i and $1/T_{1a}$ is the proton relaxation rate of pure water. An important feature of the fitting results is that any value of τ_R less than 10^{-7} s is incompatible with the data in curve *A* of Fig. 2, a result considerably different from earlier work (2). The increase in relaxation rate with field strength leading to a maximum at ~20–25 MHz may be understood, as in protein cases, by the dominance of the electron relaxation time in Eq. 4. Since the electron relaxation time is given by an equation of the form

$$\frac{1}{T_{1e}} = C\left[\frac{\tau_v}{1+\omega_S^2\tau_v^2} + \frac{4\tau_v}{1+4\omega_S^2\tau_v^2}\right], \quad (6)$$

where τ_v is another correlation time, the electron relaxation time increases with field strength. The nuclear relaxation rate will also increase until the denominator of the first term in Eq. 1, which disperses as ω_I, forces the nuclear rate to fall. That τ_R is long compared with T_{1e} is clear from the shape of the dispersion curve *A* in Fig. 2; however, an exact value of τ_R, or τ_{ex}, cannot be determined. In any case a τ_R on the order of 10^{-7} s is required, a statement that remains

true even if there is a small contribution to the data from Mn(II) ions not rigidly bound. It is interesting to note that fluorescence studies suggest torsional motions for the DNA molecule in this range (11). This long τ_R thus requires that under the conditions used to obtain curve *A*, Fig. 2, the metal ion be irrotationally bound to DNA.

The usual analysis of proton relaxation enhancement (PRE) (12) assumes no distinction among bound states or their relaxation properties. Thus,

$$1/T_1 = R_f M_f + R_b M_b + R_w, \qquad (7)$$

where R_f and R_b are the relaxation rates induced per mole of free and bound metal ion, respectively, M_f and M_b the molar concentrations, and R_w the metal free relaxation rate. At any particular frequency of interest, R_b is obtained from Fig. 2, curve *A*, and R_f obtained from Fig. 1, curve *C*. At any choice of magnetic field strength, the concentration dependence of the water proton relaxation rate may be analyzed in terms of ν_b, defined as the concentration of bound metal divided by the DNA-phosphate concentration. ν_b derived from the data in this way is shown in Fig. 3 for four choices of Larmor frequency. Though the data at one frequency appear to be self consistent, it is obvious from the different values of ν_b obtained at high concentrations that the analyses yield different quantitative results for the amount of bound ion at different frequencies. If the assumption of a single bound state were correct, the analysis would be independent of field strength. However a single $R_b(\omega)$ will not fit the data over the frequency and concentration range measured. We conclude, therefore, that the assumption of a single bound state is inaccurate, i.e. there are more than three terms in Eq. 7.

A different method has been used by Koenig and Brown and co-workers to quantitate manganese binding to macromolecules (4). These authors note that the bound ion relaxation rate is independent of magnetic field at values less than ~0.5 MHz, while the free manganese relaxation contribution suffers a significant dispersion due to the hyperfine term. They assume that all differences in the relaxation rate between 0.01 and 0.5 MHz are due to free Mn(II) ion; thus measurements at these frequencies provide an accurate measure of bound ion. Applications of the method to the Mn-DNA data for two choices of the high frequency reference point are shown in Fig. 4 as a function of total Mn(II) using the same NMRD data sets as used in construction of Fig. 3. Though these analyses are more sensitive to error in the data, it is apparent that the values of ν_b obtained are higher than in the first analysis. On the other hand, maximum values of ν_b obtained by thermodynamic methods such as equilibrium dialysis and ultracentrifugation are higher yet, ~0.4–0.45. Since six different methods of analysis including the thermodynamic methods and those shown in Figs. 3 and 4 yield different results with the assumption of a single bound state, we conclude that the assumption of a single bound state is incorrect. The difference between results of proton relaxation enhancement and equilibrium dialysis experiments has already been noted (1).

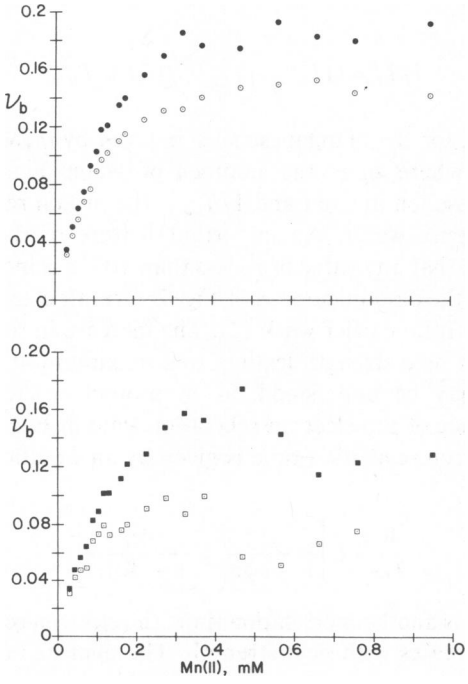

FIGURE 3 The ratio of bound Mn(II) concentration to total DNA-phosphate concentration, ν_b, as determined from the water proton relaxation data using the proton relaxation enhancement method plotted against the total Mn(II) concentration in a solution containing 0.72 mM DNA phosphate at 295 K. The different analyses were performed at 20 MHz, (○); 0.4 MHz, (●); 0.1 MHz, (■); and 0.01 MHz, (□).

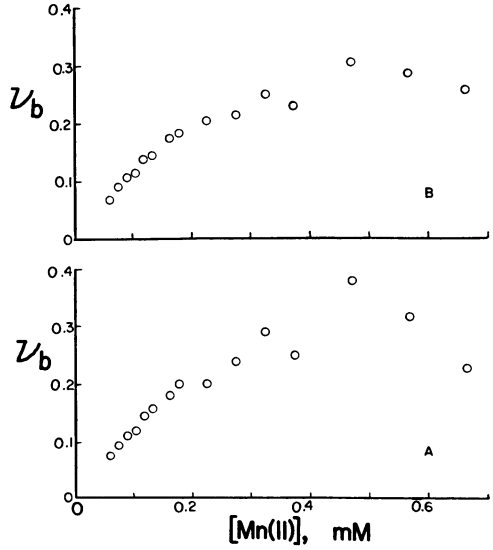

FIGURE 4 The ratio of bound Mn(II) concentration to total DNA phosphate concentration, ν_b, as determined from the water proton relaxation data using the second analysis described in the text plotted against the total Mn(II) concentration in a solution containing 0.72 mM DNA phosphate at 295 K. Relaxation rates at (*A*) 0.1 MHz, and (*B*) 0.25 MHz have been used as the high frequency reference points and the rates at 0.01 MHz have been used for the low frequency reference.

The magnetic relaxation analyses presented here strongly suggest that there are contributions to the relaxation from ions in bound states that induce dispersion curves in which the dispersion due to the hyperfine interaction is shifted to higher field relative to the aquoion case and that the dispersion due to the dipolar interaction may be shifted to lower field as in Fig. 1 *b*. The existence of such states would contribute to magnetic relaxation with a weaker field dependence between 0.01 and 0.25 MHz than that of the completely free ion (curve 1 *c*). Consequently, the second method of analysis would detect these states as bound and result in higher ν_b values. In the PRE analysis, the calculated ν_b value would increase with field strength from .01 MHz to ~0.3 or 0.4 MHz, and then decrease again as shown in Fig. 3. The ν_b values obtained by the PRE method are lower than those obtained in the second analysis because the relaxation rates due to ions in this proposed third state are smaller than those due to highly immobilized bound ions.

The dispersion spectrum shown in Fig. 1 *b* can be obtained from water protons in viscous aqueous solutions of the hexaaquomanganese(II) ion (13, 14). This information points to the presence of manganese ions in the DNA solution that are not tightly bound to the DNA, but also are not free to move as if in a purely aqueous solution. These data do not support a detailed model for the second bound environment though outer sphere hydrogen bonding between the aquoion and phosphate oxygens or simply reduced mobility of atmospherically bound ions appear to be good working hypotheses. Inner sphere ligands of DNA are not a likely source of these bound states because the immobilization would be greater than that suggested by the data. Since the thermodynamic methods yield ν_b values higher even than our second analysis, it is apparent that methods that depend on a measurement of the free ion activity report as bound a number of ions not sensed in the present experiments as irrotationally bound. It is very likely, then, that the difference is due to atmospherically bound ions, which are fully hydrated, mobile, and contribute to the relaxation as shown in Fig. 1 *c*.

An important point in this discussion is the implicit assumption that the metal ion electron relaxation time for any state of the ion is independent of concentration. Though we have no direct evidence that this assumption is inappropriate, the locally high concentration of ions at the DNA surface could cause decreases in the electron relaxation times via the electron-electron dipole-dipole interaction. A decrease in the electron relaxation time would shift the curve in Fig. 2, curve *A*, used as calibration for the analysis. It is expected, however, that the motions modulating the electron-electron dipole interactions are not very fast, being determined by diffusion of the aquoion complex or possibly by rotation of the DNA molecule. Thus, the effects of the interaction on T_{1e} would be dispersed at fields greater than 1–10 MHz and the results of the PRE analysis at 20 MHz would yield ν_b values at least as high as those at lower field strengths. Since this is not observed in Fig. 3, the electron-electron interaction appears to be minor.

The existence of multiple binding sites raises the question of analytical accuracy at any choice of field strength. Inspection of Fig. 1 indicates that measures of the irrotationally bound ion are most sensitive at the relaxation rate maximum near 25 MHz. Thus, the PRE analysis at 20 MHz is most suitable for examining the irrotational binding of Mn(II) to DNA although even this data reflects some atmospheric binding in the bound domain. The characteristics of the binding are better visualized if the data of Fig. 3 are represented in a Scatchard plot shown in Fig. 5. To make this plot, the concentration of free ion was taken to be the total number of moles of nonsite-bound ion divided by the total sample volume and will be referred to as $\overline{M}_f$. The small curvature in Fig. 5 suggests that the binding cannot be described by a simple mass action law for one binding site because in that case

$$\nu_b/\overline{M}_f = K_0(n - \nu_b), \tag{8}$$

where $\nu_b = M_b/P$ is molar concentration of site bound ions over molar concentration of DNA phosphate, $\overline{M}_f$ is the molar concentration of free ions, n is the fraction of DNA mononucleotides which can bind the metal, and K_0 is the association equilibrium constant of Mn(II) at the site and the Scatchard plot should be a straight line of slop K_0. A curved (concave up) Scatchard plot generally means either that there is negative cooperativity in the binding or that there are multiple binding sites with different binding affinities. Thus, three binding analyses have been applied

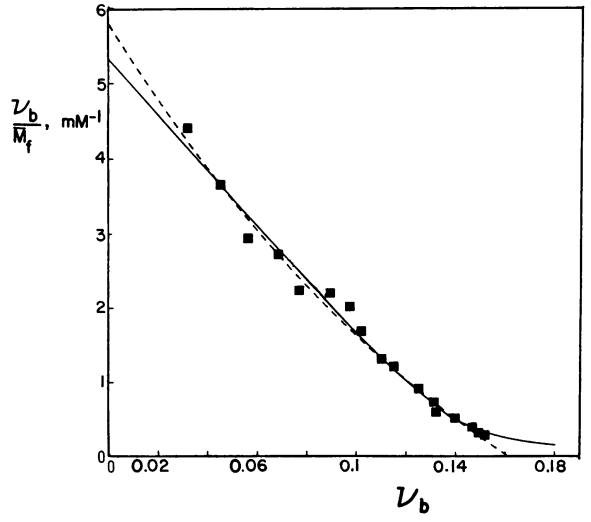

FIGURE 5 Scatchard representation of Mn(II)-DNA binding data taken from Fig. 3 resulting from proton relaxation enhancement analysis of water proton relaxation data obtained at 20 MHz. $\overline{M}_f$ is the number of moles of Mn(II) that is determined to be unbound divided by the sample volume. The dashed curve was calculated using Eq. 10 with the parameter values in Appendix *B* and the solid curve was calculated using Eq. 11 with the parameter values of Appendix *C*.

to the data of Fig. 5. The first analysis assumes a single binding site and a negative binding cooperativity in which the free energy of binding increases linearly with the extent of binding. In this case K_0 in Eq. 8 is replaced with

$$K_0 \exp(-W\nu_b), \tag{9}$$

where W reflects in some way the strength of the cooperativity. This type of behavior is like that obtained from a Poisson-Boltzmann analysis, in which the effective DNA surface charge is assumably reduced linearly with the extent of cation binding (15). Of course, assuming that bound cations, whether site or atmospherically bound, are the only ions effective in reducing effective surface charge is clearly not rigorous and herein lies one approximation of this approach. The best values obtained for K_0, W, and n by fitting the data of Fig. 5 to the combination of Eqs. 8 and 9, i.e.

$$\nu_b/\overline{M}_f = K_0(n - \nu_b)\exp(-W\nu_b) \tag{10}$$

are given in Appendix B and the fit is shown in Fig. 5 as the dashed line.

Another analysis applied to the curvature of Fig. 5 assumes two independent Mn(II) binding sites. In that case

$$\nu_b/\overline{M}_f = \frac{K_1 n_1}{1 + K_1\overline{M}_f} + \frac{K_2 n_2}{1 + K_2\overline{M}_f}. \tag{11}$$

This model assumes that the Mn(II) ion induced relaxation is the same in both bound states. The best-fit parameters for this analysis are in Appendix C and shown as the solid line in Fig. 5. Statistically, the two calculated fits shown in Fig. 5 are equally accurate.

The final binding analysis applied to the data involved theoretically estimating the concentration of unbound Mn(II) ion near the surface of the DNA molecule, $M_f(a)$, which can then be used in place of $\overline{M}_f$. Manning's condensation theory (16) was used to determine ν_c, the moles of ions per mole of DNA phosphate group "condensed" into a cylindrical shell of volume V_P about the DNA molecule. Once ν_c is known $M_f(a)$ is given by

$$1{,}000(\nu_c - \nu_b)/V_P$$

in moles per liter if V_P is in milliliters per mole-P and the data can be replotted as in Fig. 6 for V_P = 646 ml/mol-P (the value appropriate for excess 1:1 salt) and C_1 = 10 mM the concentration of tetrabutylammonium chloride. ν_c is determined from the equation

$$\nu_c/M_f(\infty) = 1{,}570\ V_p^{-1}\ C_1^{-2}\ (1 - 5.3\nu_c + 6.9\nu_c^2), \tag{12}$$

(16) where $M_f(\infty)$ is the concentration of Manganese(II) far from the DNA molecule. $M_f(\infty)$ is obtained in terms of ν_c and known quantities by observing that the total moles of Mn(II) ion in V_p plus the total moles free in solution is equal to the total added quantity of Mn(II), M_T

$$\nu_c P + M_f(\infty)\,V_s = M_T,$$

where P is the total number of moles of DNA phosphate and V_s is the volume of the sample. Solving for $M_f(\infty)$ and substitution in Eq. 12 results in a third power polynomial in ν_c, which may be numerically solved for its physically sensible roots by the Newton-Ralphson method.

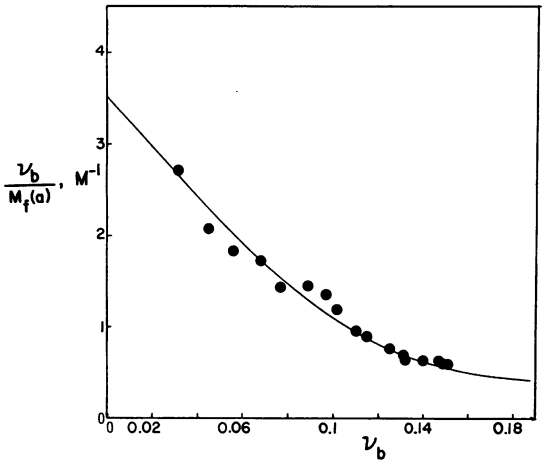

FIGURE 6 Data of Fig. 5 after correction of the Mn(II) concentration at the surface of the DNA molecule using the counterion condensation model as described in the text so $\overline{M}_f$ in Fig. 5 is replaced here by $M_f(a)$. The solid curve is calculated from the two binding sites model of Eq. 11 with the parameters in Appendix D.

If this condensation correction accurately interprets the counterion accumulation, then the biphasic nature of Fig. 6 indicates that there must be two distinct binding sites with very different equilibrium constants. The best fit values of K_1, K_2, n_1, and n_2 are given in Appendix D and the solid curve in Fig. 6 is the resulting calculation.

All three binding analyses predict one strong binding site with values of n between 0.11 and 0.162 (Appendix B–D). Kearns and co-workers have reported that a maximum of 15% of the condensed Mn(II) ions are directly coordinated to phosphate oxygen atoms based on ^{31}P relaxation and shift measurements (5), which would correspond to a maximum value of n of ~0.06. The results of this work as well as those of others (6, 17) suggest additional sites. These extra sites are more likely to be on the bases than on deoxyribose groups. There is strong evidence for the binding of manganese to guanine bases (6, 18–22). In particular, Steenwinkel's work (6), where the extent of binding to DNA is observed to vary directly with G-C content is complimented by Raman and crystallographic observations (18–20, 22) that Mn(II), among other metals, appears to interact with purine bases but not pyrimidines. Furthermore, since we have shown that the PRE analysis at 20 MHz detects primarily highly immobilized bound ions, the data here suggest that the strong manganese binding is a specific interaction rather than electrostatic.

Existence of a second and weak site that is more abundant is suggested by the curvature of Fig. 6 although this could be an artifact due to the use of condensation theory in the analysis or to contributions to the relaxation arising from atmospherically bound ions.

Mn(II) is not found at high concentrations in most living systems but is often used as a model or probe ion for magnesium or calcium. Though ^{25}Mg NMR has demonstrated considerable binding of magnesium ion to DNA (23; Mie et al., unpublished manuscript), some of which is interpreted to be of a first coordination sphere type because of the magnitude and temperature dependence of the line width changes, an indirect assessment is offered by the proton relaxation induced by Mn(II). Fig. 7 shows the results of two competition measurements involving calcium and magnesium monitored at 20 MHz. These data demonstrate that the two ions have completely equivalent effect on the Mn(II) contributions to the water relaxation rates. If we assume that every displaced Mn(II) ion is replaced by a magnesium (calcium) ion and that if the manganese sites are different from the magnesium sites, they are sufficiently close to permit occupancy by only one ion or the other, then

$$K_{Mg} = \frac{[Mg]_b(1 + K_{Mn}[Mn]_f)}{[Mg]_f(n[P] - [Mg]_b)}, \qquad (13)$$

where K_{Mg} and K_{Mn} are the magnesium and manganese association binding constants, respectively, $[Mg]_f$ and $[Mn]_f$ are the free concentrations of Mg and Mn, $(Mg)_b$ is the bound concentration of magnesium, $[P]$ is the concentration of DNA phosphate, and n is the ratio of bound manganese to DNA phosphate before any magnesium (or calcium) has been added. The value of $K_{Mg,Ca}$ so obtained is a maximum because displaced manganese does not necessarily imply replacement by bound magnesium or calcium.

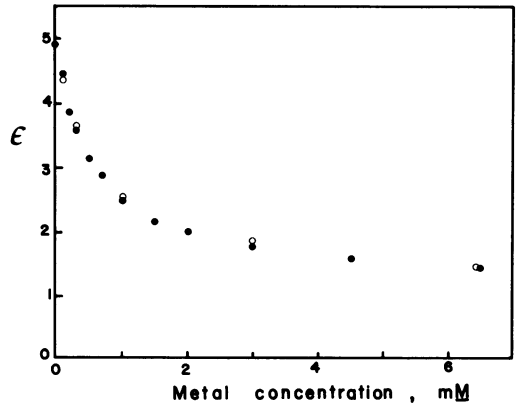

FIGURE 7 Water proton relaxation rate enhancement (ϵ) due to DNA in solution containing 0.30 mM Mn(II) and 0.72 mM DNA phosphate at 295 K and a range of concentrations of magnesium (●) or calcium (○). ϵ is the ratio of the measured relaxation rate and that expected for a pure aqueous solution of 0.3 mM $MnCl_2$. $\epsilon = 1$ corresponds to all Mn(II) being free as the hexaaquoion.

Applying Eq. 13 to the data in Fig. 7 permits the conclusion that the magnesium and calcium association constants are about half that for manganese, which supports the earlier suggestions that manganese ions are involved in site-specific interactions with DNA.

Fig. 8 shows the results of a competition experiment analogous to that in Fig. 7, except that monovalent ions sodium and lithium are used instead of magnesium and calcium. The data show that a given lithium concentration drives the proton relaxation enhancement to a lower value than does an equivalent sodium concentration indicating that lithium associates with DNA more effectively than does sodium. No mechanism for this behavior is suggested by the data, but aspects of sodium and lithium chemistry allow some speculation: (*a*) since the lithium aquoion is more tightly hydrated than the sodium aquoion (24) that does not interact with DNA in the first coordination sphere (3), it is unlikely that inner sphere bonds are responsible for the stronger affinity of lithium ion for DNA; (*b*) since sodium ion is usually observed to bind to cation exchange resins more strongly than lithium (24), nonspecific electrostatic considerations are unlikely to explain the DNA competition; (*c*) a lithium ion with only one hydration layer filled may be small enough to slip into the minor groove of the B form of DNA where the electrostatic potential of DNA is low (25). The lithium NMR may be particularly informative about the interaction as could the relaxation dispersion of lithium.

CONCLUSION

The wealth of information contained in the water proton NMR dispersion spectrum has been used in this study to show that Mn(II) ion may be irrotationally bound to the DNA molecule. The binding is most likely inner sphere and may involve one of the guanine or cytidine bases. Extensive analysis of the manganese ion titration experiment using several analytical approaches has provided evidence of bound environments of the divalent ion in

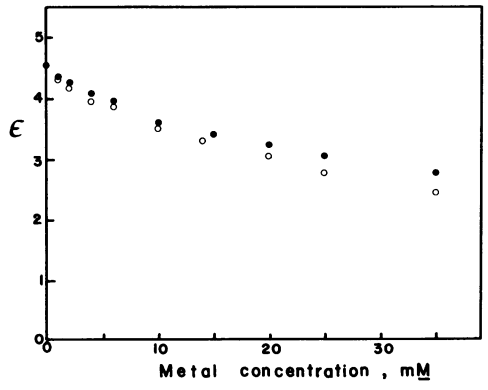

FIGURE 8 Water proton relaxation rate enhancement due to DNA in a solution containing 0.27 mM Mn(II) and 0.72 mM DNA phosphate at 295 K and a range of sodium and lithium ion concentrations.

which it is not completely immobilized, but its motion is only partially restricted. The data obtained as a function of magnetic field strength demonstrated that analysis for the irrotationally bound ion is best carried out at 20 MHz. Application of an electrostatic theory to assist the ion binding analysis permits deconvolution of the binding isotherm in terms of two types of sites of different affinity. Competition experiments with magnesium and calcium for the Mn(II) interactions have demonstrated that these ions may eliminate the specific Mn(II)-DNA interactions though the affinity of DNA for these ions is approximately half that for the Mn(II) ions.

Received for publication 30 May 1985 and in final form 28 March 1986.

APPENDIX

(*A*) Parameters for calculating solid curve of Fig. 2 from Eqs. 1–6

$q = 5$ $\quad \tau_R = 1.7 \times 10^{-7}$ s

$r = 2.74$ Å $\quad \tau_{ex} = 7.6 \times 10^{-7}$ s

$A = 0.82$ MHz $\quad \tau_v = 1.4 \times 10^{-11}$ s

$C = 2.7 \times 10^{-19}\ s^{-2}$

(*B*) Parameters for calculating dashed curve of Fig. 5 from Eq. 10

$K_0 = 35.6 \times 10^3\ M^{-1}$ $\quad W = 3$ $\quad n = 0.162$

(*C*) Parameters for calculating solid curve of Fig. 5 from Eq. 11

$K_1 = 38 \times 10^3\ M^{-1}$ $\quad K_2 = 1 - 0.2 \times 10^3\ M^{-1}$*

$n_1 = 0.14$ $\quad n_2 = 0.06 - 0.3$*

(*D*) Parameters for calculating solid curve of Fig. 6 from Eq. 11

$K_1 = 30\ M^{-1}$ $\quad K_2 = 0.2 - 0.65\ M^{-1}$*

$n_1 = 0.11$ $\quad n_2 = 1 - 0.35$*

REFERENCES

1. Rose, D. M., M. L. Bleam, M. T. Record, Jr., and R. G. Bryant. 1980. ^{25}Mg NMR in DNA solutions: dominance of site binding effects. *Proc. Natl. Acad. Sci. USA.* 77:6289–6292.
2. Granot, J., and D. R. Kearns. 1982. Interactions of DNA with divalent metal ions. II. Proton relaxation enhancement studies. *Biopolymers.* 21:203–218.
3. Anderson, C. F., M. T. Record, Jr., and P. A. Hart. 1978. Sodium-23 NMR studies of cation-DNA interactions. *Biophys. Chem.* 7:301–316.
4. Hallenga, K., and S. H. Koenig. 1976. Protein rotational relaxation as studied by ^{1}H and ^{2}H magnetic relaxation. *Biochemistry.* 15:4255–4264.
5. Granot, J., Feigon, J., and D. R. Kearns. 1982. Interactions of DNA with divalent metal ions. I. ^{31}P-NMR studies. *Biopolymers.* 21:181–201.
6. Steenwinkel, R. V., F. Campagnari, and M. Merlini. 1981. Interaction of Mn^{2+} with DNA as studied by proton-relaxation enhancement of solvent water. *Biopolymers.* 20:915–923.
7. Solomon, I. 1955. Relaxation processes in a system of two spins. *Phys. Rev.* 99:559–565.
8. Solomon, I., and N. Bloembergen. 1956. Nuclear magnetic interactions in the HF molecule. *J. Chem. Phys.* 25:261–266.
9. Bloembergen, N., and L. O. Morgan. 1961. Proton relaxation times in paramagnetic solutions. Effects of electron spin relaxation. *J. Chem. Phys.* 34:842–850.
10. Rubenstein, M., Baram, A., and Z. Luz. 1971. Electronic and nuclear relaxation in solutions of transition metal ions with spin $S = 3/2$ and $5/2$. *Mol. Phys.* 20:67–80.
11. Thomas, J. C., Allison, S. A., Appellof, C. J., and J. M. Schurr. 1980. Torsion dynamics and depolarization of fluorescence of linear macromolecules. II. Fluorescence polarization anisotropy measurements on a clean viral ϕ29 DNA. *Biophys. Chem.* 12:177–188.
12. Burton, D. R., Forsen, S., Karlstrom, G., and R. A. Dwek. 1979. Proton relaxation enhancement (PRE) in biochemistry: a critical survey. *Prog. NMR Spectros.* 13:1–45.
13. Hausser, R., and F. Noack. 1964. Kern magnetische Relaxation und Korrelation in Zwei-Spin-Systemen. *Z. Phys.* 182:93–110.
14. Kennedy, S. D., and R. G. Bryant. 1985. Proton magnetic relaxation in aqueous glycerol solutions containing manganese(II) ion. *Magn. Res. Med.* 2:14–19.
15. Gross, L. M., and U. P. Strauss. 1966. *In* Chemical Physics of Ionic Solutions. B. E. Conway and R. G. Barradas, editors. John Wiley & Sons, New York.
16. Manning, G. S. 1978. The molecular theory of polyelectrolyte solutions with application to the electrostatic properties of polynucleotides. *Q. Rev. Biophys.* 11:179–246.
17. Eisinger, J., F. Fawaz-Estrup, and R. G. Shulman. 1965. Binding of Mn^{2+} to nucleic acids. *J. Chem. Phys.* 42:43–53.
18. Jack, A., J. E. Ladner, D. Rhodes, R. S. Brown, and A. Klug. 1972. A crystallographic study of metal-binding to yeast phenylalanine transfer RNA. *J. Mol. Biol.* 111:315–328.
19. Rimai, L., and M. E. Heyde. 1970*a*. An investigation by Raman spectroscopy of the base-proton dissociation of ATP in aqueous solution and the interactions of ATP with Zn and Mn. *Biochem. Biophys. Res. Commun.* 41:313–320.
20. Rimai, L., Heyde, M. E., and E. B. Carew. 1970*b*. Effect of divalent metal ion binding on the Raman spectrum of ATP in aqueous solution. *Biochem. Biophys. Res. Commun.* 38:231–237.
21. Clement, R. M., J. Sturm, and M. P. Duane. 1973. Interaction of metallic cations with DNA VI. Specific binding of Mg and Mn. *Biopolymers.* 12:405–421.
22. Gellert, R. W., and R. Bau. 1979. X-ray structural studies of metal-nucleoside and metal-nucleotide complexes. *In* Metal Ions in Biological Systems. H. Sigel, editor. Marcel Dekker Inc., New York. 8:1–55.
23. Rose, D. M., C. F. Polnaszek, and R. G. Bryant. 1982. ^{25}Mg-NMR investigations of the magnesium ion-DNA interaction. *Biopolymers.* 21:653–664.
24. Cotton, F. A., and G. Wilkinson. 1962. Advanced Inorganic Chemistry. Interscience Publishers, Inc., John Wiley & Sons, New York. Chs. 2 and 6.
25. Perhia, D., Pullman, A., and B. Pullman. 1979. Molecular electrostatic potential of the B-DNA Helix. V. Poly (dG · dC) and Poly (dA · dT). Intern. *J. Q. Chem. Quant. Biol. Symp.* 6:353–363.

*The best-fit values not well determined by data.